# Customizable Island-Bridge Structures for Stretchable Displays

*Yangyang Wang, Hao Hang, Chunxiao Gu, Huihui Meng, Zhimin Yan and Wangfeng Xi*
**Visionox Technology Inc., Gu'an, Hebei Province, China**

## Abstract
***In this paper, we fabricated a variety of stretchable samples using twenty kinds of bridges to investigate the influences of design parameters (such as line width, radius, total arc length, etc.) on stretchability. The failure characteristics were further verified at both large arc apexes and small arc connection sites by simulation. A dynamic stretchable AMOLED module with a stretch of more than 15% was successfully obtained.***

## Author Keywords
Stretchable electronics; Stretchability; AMOLED; Island-bridge.

## 1. Introduction
As the ultimate display form of next-generation technology, stretchable displays that retain their electronic functions under large tensile strains are highly alluring [1]. Indeed, nowadays we are witnessing the emergence of dazzling stretchable display prototypes by several display companies. These displays are designed as a hybrid system consisting of rigid islands and serpentine-shaped stretchable wirings, also known as the island-bridge structures [2]-[5]. In this hybrid system, rigid islands remain unaffected by deformations during expansion. In contrast, stretchable wiring can cover the total deformation of the system, which means the stretchability and stability of the bridge should be sufficiently stable to withstand the total deformation of the system [6]. Stretch reliability is a crucial evaluation indicator for stretchable technology, and designing devices capable of withstanding high levels of stress poses significant challenges. It is particularly important to examine the relationship between the bridge's design and process parameters and its final stretchable properties, which can assist researchers in creating high-performance island-bridge structures that can be produced with production-ready and highly stable stretchable displays. In this study, we demonstrated a variety of stretchable samples based on twenty kinds of stretchable bridges using design of experiments (DOEs). We thoroughly investigated how design and process parameters, such as line width, edge width, arc angle, radius, linear length, total arc length, and the layers of metal wiring, affect the stretchability of the integral integration system. Simulation was used to further verify the failure characteristics of the stretchable bridges. The above island-bridge structure was used to obtain a dynamic stretchable active matrix organic light emitting diode (AMOLED) module that can stretch more than 15%.

## 2. Results and Discussions
### *2.1 Island-bridge Structure Design Parameters*
To streamline the process, we prepared a range of stretchable samples based on simple bridge designs (shape-C, shape-S, and double-line shape-C) without thin-film transistors, as shown in Figure 1(a). We developed both single (only M3) and double (including M3 and M4) metal layers to assess the impact of the metal wiring layers on the tensile properties of the samples. Several design factors, including line width, edge width, arc angle, radius, linear length and total arc length, were designed for twenty kinds of DOEs to evaluate their stretchability. It should be noted that the theoretical maximum tensile strain (ε) is defined as

$$\varepsilon = \frac{L-L_0}{L_0} \times 100\% \quad (1)$$

Where $L$ is the total arc length, $L_0$ is the distance between two islands. The total arc length can be calculated by Equation 2:

$$L = 2 \times L_1 + \frac{2\times\alpha\times\pi\times r}{180} + \frac{\theta\times\pi\times R}{180} + 2 \times L_2 \quad (2)$$

Where $R$ and $r$ correspond to the radii of the large and small arcs, $\theta$ and $\alpha$ represent the arc angles of the large and small arcs, respectively, as shown in Figure 1(b). Figure 1(c)-(e) show the influence factors explored in this paper, where *a1* is the line width, *a2* is the edge width, *a3*, *a4*, and *a5* are the line distance, center angle of large arc, and radius of shape-C large arc, respectively. *b1*, *b2*, and *b3* are the linear length, arc angle and radius of shape-S, respectively.

The structures of twenty kinds of DOEs are depicted in Figure 2(a). Specifically, shape-C is employed for DOE-1 to DOE-11, shape-S for DOE-12 to DOE-17, and double-line shape-C for DOE-18 to DOE-20. According to Equations 1 and 2, we calculated the theoretical maximum strain of the aforementioned twenty kinds of DOEs, and the relevant results are shown in Figure 2(b) and Table 1. The actual measured maximum strain results are also displayed in Figure 2(b). The outcomes demonstrate a favorable agreement between the experimental and the theoretical strains while exhibiting a strong correlation with the total arc length. That is, designs with larger arc lengths are favored for attaining heightened levels of stretchability. The as-fabricated samples were subjected to mechanical tests in order to further validate their tensile fatigue characteristics, specifically focusing on shape-C (DOE-8, DOE-9), shape-S (DOE-16, DOE-17), and double-line (DOE-18). This selection was made to assess the relative resistance of these shapes and changes in metal layers. Relative resistance during stretching and releasing cycles under uniaxial tensile strains is illustrated in Figure 2(c). It can be observed that all samples undergo cyclic stretching (1000 times) at a strain of 15%, with a resistance change rate below 1%. This indicates excellent tensile stability of the

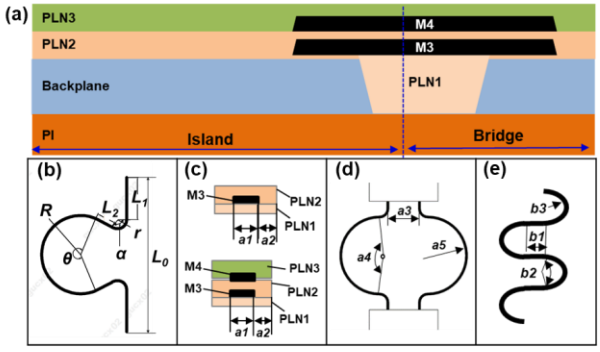


**Figure 1.** (a) Schematic of stretchable samples based on the island-bridge structure. Schematic of the geometry of the theoretical maximum strain (b), single (up) and double (bottom) metal layers (c), shape-C design parameters (d), and shape-S design parameters (e).


*ISSN 0097-996X/25/5603-2022-$1.00 © 2025*

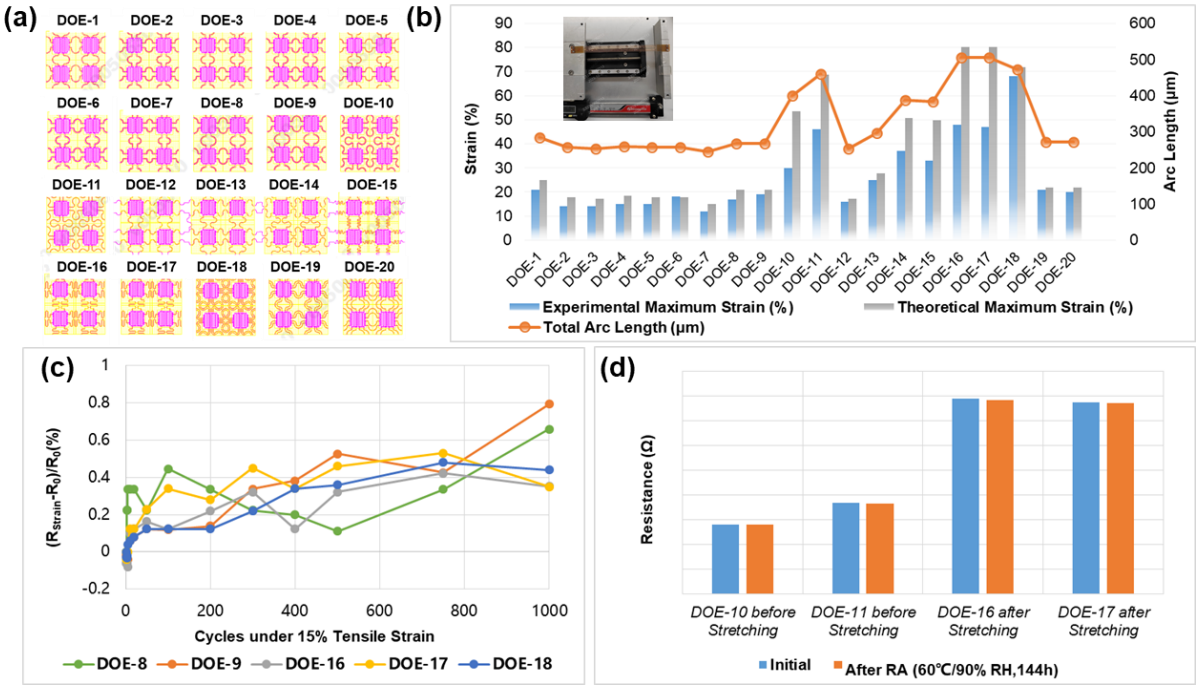


**Figure 2.** (a) Structural diagrams of twenty kinds of island-bridge designs. (b) The theoretical and experimental maximum strain of twenty kinds of DOEs, inset: photograph of a stretchable sample. (c) Resistance stability of the samples during repeatable 15% uniaxial tensile strain and release. (d) Resistance change of the samples before and after reliability (RA) test.

**Table 1.** Summary of influencing parameters and mechanical properties of a variety of stretchable samples.

| DOE | Type | Line width | Edge width | Linear length | Arc angle | Radius | Total arc length (μm) | Experimental maximum strain (%) | Theoretical maximum strain (%) | Results (to obtain high maximum strain) |
|---|---|---|---|---|---|---|---|---|---|---|
| 1 | C | Medium | Medium | / | Small | Large | 285.3 | 21 | 25.08 | Choose large radius |
| 2 | C | Medium | Medium | / | Small | Medium | 256.7 | 14 | 17.93 | |
| 3 | C | Small | Medium | / | Small | Medium | 254.1 | 14 | 17.28 | Choose small line width |
| 4 | C | Large | Medium | / | Small | Medium | 259.3 | 15 | 18.58 | |
| 5 | C | Medium | Small | / | Small | Medium | 256.7 | 15 | 17.93 | Edge width has less effect |
| 6 | C | Medium | Large | / | Small | Medium | 256.7 | 18 | 17.93 | |
| 7 | C | Medium | Medium | / | Small | Small | 245.3 | 12 | 15.08 | Choose large radius, and there is negligible differences in metal layers |
| 8 | C | Medium | Medium | / | Small | Large | 268.1 | 17 | 20.78 | |
| 9 | C-bilayer | Medium | Medium | / | Small | Large | 268.1 | 19 | 20.78 | |
| 10 | C | Medium | Medium | / | Large | Medium | 399.4 | 30 | 53.60 | Choose large arc angle |
| 11 | C | Small | Small | / | Large | Medium | 460.0 | 46 | 68.75 | Shape-C best |
| 12 | S | Small | Small | Small | Small | Large | 253.3 | 16 | 17.08 | Choose large linear length |
| 13 | S | Small | Small | Medium | Small | Large | 296.1 | 25 | 27.78 | |
| 14 | S | Small | Small | Medium | Medium | Super Large | 387.5 | 37 | 50.63 | Choose large radius and arc angle, and there is little difference in metal layers |
| 15 | S | Small | Small | Medium | Small | Small | 383.6 | 33 | 49.65 | |
| 16 | S | Small | Small | Large | Small | Medium | 506.3 | 48 | 80.33 | |
| 17 | S-bilayer | Small | Small | Large | Small | Medium | 506.3 | 47 | 80.33 | |
| 18 | Double-line | Small | Small | / | Large | Medium | 472.3 | 68 | 71.83 | Choose large total arc length, the rule is the same as the single-line |
| 19 | Double-line | Small | Small | / | Small | Small | 272.4 | 21 | 21.85 | |
| 20 | Double-line | Small | Small | / | Small | Large | 272.4 | 20 | 21.85 | |

| (a) Type | Shape-C | | | Shape-S | | Double-line |
|---|---|---|---|---|---|---|
| DOE | DOE-3 | DOE-7 | DOE-11 | DOE-12 | DOE-13 | DOE-18 |
| Theoretical deformation under stress (%) | 2.68 | 5.95 | 0.48 | 3.22 | 1.75 | 1.55 |
| Simulation diagram | 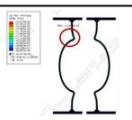 | 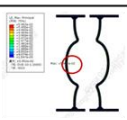 | 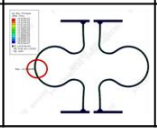 | 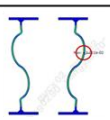 | 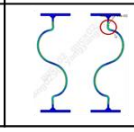 | 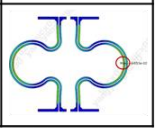 |

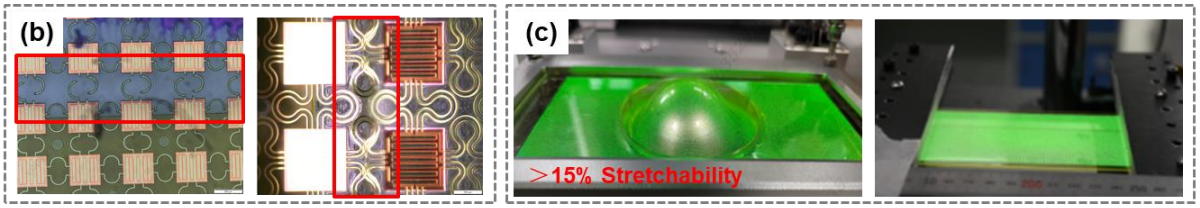


**Figure 3.** (a) Simulation results of failure sites of island-bridge structures when stretch to 10%. The red ellipses in the simulation diagram represent the locations with maximum deformation. (b) Microscopy photographs show that the failure location (red frame) is concentrated at the apex of the large arc and the connection of the small arc. (c) Photographs of the AMOLED modules with a more than 15% stretchability during undergoing bump stretching (left) and plane stretching (right).

island-bridge structure regardless of the C or S shape, even for double-line and metal single layer or bilayer configurations. In addition, taking DOE-10, DOE-11, DOE-16 and DOE-17 as examples, the samples before and after stretching remain unchanged when placed in thermal humidity storage test (60 ℃, relative humidity (RH) of 90%, for a duration of 144 hours), highlighting the exceptional reliability of our stretchable samples, as shown in Figure 2(d).

The correlation between design parameters (such as line width, edge width, arc angle, radius, linear length and total arc length) and theoretical/actual maximum strain is presented in Table 1. The results reveal that a larger radius, arc angle and linear length and a smaller line width contribute to obtaining a higher total arc length and achieving greater strain. The impact of edge width on strain is minimal. Furthermore, the impact of metal layers on stretchability is almost negligible when the arc length remains constant. For instance, comparing DOE-9 with DOE-8 or DOE-17 with DOE-16 shows that metal bilayer exhibits similar properties to single metal layer regardless of the C or S shape. In terms of double-line structural design for maximizing arc length and achieving optimal mechanical properties following the same rule as single-line structures applies. In summary, during the actual design process of an island-bridge structure, it is important to comprehensively consider these parameters in order to obtain maximum arc length which not only increases overall stretchability but also strengthens weak points against greater stress deformation.

### *2.2 Failure Mechanism of Island-bridge Structure*

To further investigate the failure mechanism of the island-bridge structure, we conducted simulations to verify the failure locations of different bridges. As depicted in Figure 3(a), the results from six kinds of DOEs indicate that when subjected to a 10% stretch, the bridges experience maximum stress and deformation at the apex of the large arc and connection point of the small arc. This conclusion is also supported by optical microscopes (Figure 3(b)). Hence, during the actual design process, it is essential to focus on reinforcing the aforementioned weak points in order to enhance tensile stability.

### *2.3 Stretchable AMOLED Module*

In order to validate the feasibility of as-designed island-bridge structure, we developed a stretchable AMOLED module based on DOE-1 as an example. Figure 3(c) demonstrates that the visualized stretchable display functions reliably without any breakage or defects even under more than 15% convex and plane tensile strains. The next step involves incorporating island-bridge structures with extended arc lengths (such as DOE-11, DOE-16, and DOE-18) as design principles for the development of stretchable displays with improved stretchability.

## 3. Conclusion

We successfully fabricated various stretchable samples using twenty kinds of DOEs to evaluate design and process parameters, such as line width, edge width, arc angle, radius, linear length, total arc length, and metal layers on the integral integrated system's stretchability. The results indicate a robust correlation between the maximum strain in stretchable samples and the arc length of bridges. In other words, designs with larger arc lengths are favored for attaining heightened levels of stretchability. Failure characteristics were verified at both large arc apexes and small arc connection sites. Finally, a dynamic stretchable AMOLED module with a stretching rate of more than 15% was obtained based on the island-bridge structure of DOE-1.

## 4. References

1. Qian Yang, et al. Design of Stretchable AMOLED Display with Transitional Area, SID DIGEST 51, 1142 (2020)
2. Chengliang Wang, et al. High Resolution Stretchable Micro-LED Displays, SID DIGEST 53, 521 (2022)
3. Hejin Wang, et al. Structure Optimization of Stretchable AMOLED based on LTPS TFT, SID DIGEST 55, 2033 (2024)
4. Masashi Miyakawa, et al. Highly Stretchable Liquid Metal-based Deformable Micro-LED Displays, SID DIGEST 55, 1317 (2024)

5. Jong-Ho Hong, et al. Highly Stretchable and Shrinkable AMOLED for Free Deformation, SID DIGEST 54, 1041 (2023)
6. Myung Sub Lim, et al. Evaluation Method and Results for Measuring Stretchability of Two Dimensional Stretchable Displays, SID DIGEST 55, 1324 (2024)